IOP Publishing Journal of Micromechanics and Microengineering
J. Micromech. Microeng. **28** (2018) 095001 (11pp) https://doi.org/10.1088/1361-6439/aac221

Compensation of frequency split by directional lapping in fused quartz micro wineglass resonators

Yusheng Wang, Mohammad H Asadian and Andrei M Shkel

University of California, Irvine, CA 92697, United States of America

E-mail: yushengw@uci.edu, asadianm@uci.edu, and ashkel@uci.edu

Received 11 January 2018, revised 4 April 2018
Accepted for publication 3 May 2018
Published 21 May 2018

Abstract

We present, for the first time, a permanent structural asymmetry compensation method for fused quartz micro wineglass resonators. Using the technique, we demonstrated a near six times reduction of structural asymmetry ($n = 2$ wineglass mode), culminating in reduction of the frequency split from 41 to 7 Hz. This is an iterative process. In each iteration, the structural asymmetry was first identified by measuring the mode shape of the resonators. Then, directional lapping was performed with specially designed lapping fixtures to accurately control the lapping angle down to 1°. Analytical predictions and numerical simulations were conducted to study the structural asymmetry phenomenon and the effects of compensation on the quality factor of the structure, showing the ability of this process to reduce the structural asymmetry, while not affecting the overall quality factor of the resonators.

Keywords: frequency split reduction, directional lapping, wineglass resonators, structural asymmetry, quality factor

(Some figures may appear in colour only in the online journal)

1. Introduction

Macro-scale hemispherical resonator gyroscopes have demonstrated high structural symmetry, low energy loss, and remarkable shock resistance, [1–3], inspiring the development of wafer-level fabrication of micro-scale 3D structures for environmentally robust vibratory MEMS gyroscopes. Micro devices fabricated from polysilicon [4], polycrystalline diamond [5], bulk metallic glass (BMG) [6], and fused quartz [7, 8], showed their feasibility. For macro-scale devices, high structural symmetry is achieved through a combination of precision machining and post-process trimming, [1]. This approach is typically not available for micro-scale fabrication. The achievement of high structural symmetry, i.e. low frequency split, remains to be a priority for making progress in realization of precision MEMS devices. Innovative compensation methods are necessary to reduce the frequency split to achieve high performance sensors, such as gyroscopes operating in rate-integrating and mode-matched angular rate modes, [9].

A method commonly used in MEMS to compensate for frequency split of a resonator is by applying electrostatic forces, modifying the effective stiffness associated with the structural mode, [10, 11]. The accuracy of the compensation depends on the accuracy of control of the tuning voltages. However, due to limitations of electronics, it is challenging to control the large magnitude of tuning voltage with required high precision. Therefore, only devices with small initial frequency split can be accurately compensated, requiring only relatively low tuning voltages, [12]. Micro-fabrication of ideally symmetric devices would be preferable, but not realizable in practice. In most cases, a permanent modification of devices is necessary for reducing large as-fabricated frequency splits, followed by a relatively low tuning voltage, and therefore a high electrostatic tuning accuracy.

The mass perturbation method has been widely applied to permanently compensate for the frequency split, where mass-points are added or subtracted from devices to change their overall mass distribution and therefore to reduce the frequency split of the structure, [13]. In [14], the laser ablation

 © 2018 IOP Publishing Ltd Printed in the UK

method was applied to single-ring silicon resonators, demonstrating the reduction of the out-of-plane frequency split from 26 Hz to 7 Hz, and in-plane frequency split from 3 Hz to 1 Hz. However, the quality factor was reported to decrease due to creation of amorphous silicon and micro-cracking in the vicinity of ablation. Besides, a significant amount of debris was created at both sides of the ablated trenches. In [15], reservoirs and gold pads were introduced on spokes of multi-ring resonators for subsequent deposition of localized masses during post-processing. Frequency split reduction from 30 Hz to 80 mHz was demonstrated on silicon multi-ring resonator without affecting the quality factor of the device. The method of selectively removing material for tuning structures is attractive, but is not currently compatible with 3D shell resonators. In [5], tabs coated with Cr/Au were co-fabricated at the rim of a diamond hemispherical resonator. The coated metal was selectively ablated by laser to reduce the frequency split of the device. The frequency split reduction from 35.5 Hz to 0.35 Hz was experimentally demonstrated. However, it was noticed that the thick metal coating may reduce the overall quality factor of the resonator. In [16], a high resolution micro ultrasonic machining was proposed to trim 3D micro structures. Holes with 60 μm diameter for compensation purposes were demonstrated on bird-bath shells. Surface roughness in the range of 120–150 nm was measured on sidewalls of the holes. No frequency split reduction data was reported in this study. The high surface roughness and the disturbance of the integrity of the shell structure might affect the quality factor of the devices. To the best of our knowledge, no frequency split reduction method and its effect on the quality factor for 3D structures was studied. This paper intends to fulfill this gap.

In this paper, we explore an alternative approach to the permanent frequency split reduction of fused quartz micro-glassblown wineglass resonators utilizing the directional lapping. The idea is to adjust structural asymmetry of the as-fabricated asymmetric structure by directionally lapping the rim of the shell to compensate for the structural asymmetry. The major advantage of this approach is the ability to keep the integrity of the 3D structure while compensating for the as-fabricated imperfections. This technique has the ability of preserving the overall quality factor of the resonator since it utilizes the same lapping process as in the release step of the fabrication process (described in [7]). In the proposed approach, we first determine the orientation of the asymmetry by measuring the mode shapes of the resonator. Then, the directional lapping is performed based on the information about asymmetry by aligning the lapping direction along the axis of asymmetry. A near six times of frequency split reduction has been demonstrated on $n = 2$ wineglass mode of wineglass shell resonator. The reported permanent lapping technique is envisioned as a step in a three-step fabrication sequence, where a precision shell is first fabricated, then directionally lapped, and finally fine-tuned electrostatically to achieve the desirable high symmetry.

The paper is organized as follows. In section 2.1, we will first demonstrate the effects of temperature non-uniformity during glassblowing on the symmetry of wineglass structures, which is a major source of asymmetry of the process. This

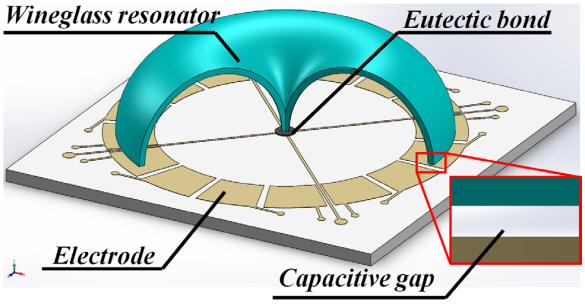

Figure 1. Schematics of a micro glassblown wineglass resonator with assembled electrodes. © (2017) IEEE. Reprinted, with permission, from [22].

will be followed by our study on effects of lapping errors on the mode shapes of the wineglass structure in section 2.2. A model of the effects of directional lapping on the change of frequency split will be discussed in section 2.3. In section 3.1, we will present a procedure for identification of asymmetry. This is followed by the process of directional lapping in section 3.2, and the directional lapping results in section 3.3. In section 4, we will present the effects of directional lapping on the quality factor of the devices by analyzing the thermo-elastic damping (TED), surface finish of lapping, and the anchor loss. The paper concludes with the discussion of results in section 5.

2. Structural symmetry analysis

2.1. Structural asymmetry during glassblowing

Micro-glassblowing technique has been developed as an approach to fabricate 3D fused quartz wineglass resonators (figure 1), [17]. In this process, a fused quartz wafer is first etched by hydrogen fluoride (HF) to create cavities for glassblowing. Then, it is bonded with another fused quartz wafer to seal the cavities. Next, the wafer stack is placed in the high-temperature furnace for glassblowing. Mechanical removal of the substrate is conducted after the blowing in order to release the devices. In this process, atomically smooth and spherical shell structures were experimentally demonstrated with the radial error less than 500 ppm, [18]. However, many sources of fabrication imperfections may cause structural asymmetry of glassblown wineglass resonators and a change of mode shapes of the resonators, including the temperature non-uniformity in the glassblowing process, the misalignment between the device and the lapping plane during the release, and a thickness variation of the device layer created during the HF wet etching, [19]. Among all these factors, the temperature non-uniformity during glassblowing is the most dominant factor. In this section, we present a relation between the temperature non-uniformity and the structural asymmetry of the wineglass resonators.

ANSYS Polyflow was used to simulate the glassblowing process. Generalized Newtonian non-isothermal flow model was applied to simulate the temperature non-uniformity. Temperature-dependent viscosity of fused quartz was approximated by Arrhenius exponential model and the parameters were extracted from [20]. In [20], the viscosity of silica was

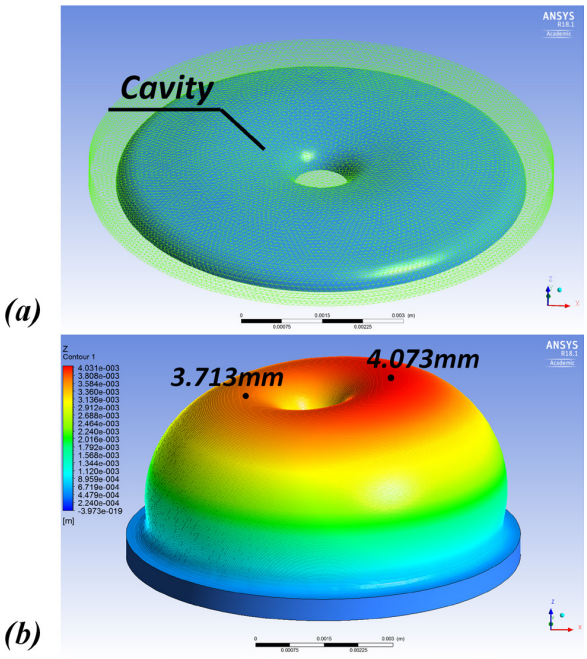

Figure 2. Shape of the model (a) before blowing, and (b) after blowing. Cavity is indicated by the solid blue part. The modeling shows a source of possible imperfections in glassblown structure, which needs to be compensated. Temperature non-uniformity in furnace during the glassblowing process resulted in asymmetry of the structure. The temperature difference between the two sides of the substrate was set to be 20 °C. The maximum deformations in height on the '+x' and '−x' side of the blown shell were 4.073 mm and 3.713 mm, respectively.

listed in a wide range of temperature from 1200 °C to 2500 °C, matching the temperature during glassblowing (around 1500 °C). In the model, thickness of the device layer before glassblowing was 100 μm, the diameter of the cavity was 7 mm, and the thickness of the cavity was 400 μm (figure 2). The average glassblowing temperature was set to be 1500 °C. The temperature difference was applied along the x-axis and the gradient was assumed to be constant. To reduce the amount of calculation, the substrate layer of the glass-to-glass stack was not included in the model and only the deformation of the device layer was simulated, since the deformation of the substrate was small compared to that of the device layer. A constant pressure difference of 4 bar between the top and bottom of the device layer was applied to model the process of glassblowing. The prediction of glassblowing result with 20 °C temperature difference between the two sides (+x and −x) of the substrate is shown in figure 2. The maximum deformation in height on the '+x' side of the blown shell was 4.073 mm and the maximum deformation in height on the '−x' side was 3.713 mm. The height difference between the two sides was calculated to be 0.36 mm. The obtained height difference was due to the viscosity difference caused by temperature gradient through the structure. It was also an indicator of structural asymmetry, which would cause the frequency split of the wineglass resonator. The relation between the temperature difference and the glassblowing height difference is presented in figure 3. The height difference would be

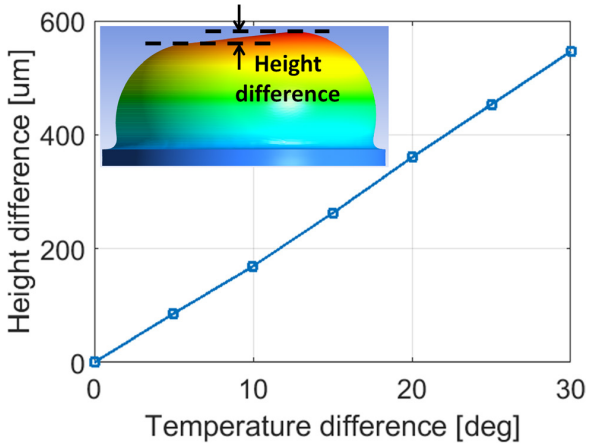

Figure 3. Relation between the temperature difference and the height difference. The inserted plot is the side view of the glassblown structure.

zero and the structure would be axisymmetric if the temperature were uniform. When temperature difference between the two sides of the die reached 30 °C, the height difference was around 0.55 mm, more than 15% of the net height of the shell structure (excluding the substrate).

2.2. Effects of lapping on asymmetry

Fabrication imperfections, such as lapping errors, will change the mode shapes of the resonator, as well as induce the frequency mismatch between the two degenerate modes, as shown in figure 4. On the left side of figure 4, the blue solid line and the red dashed line represent in the frequency domain the responses of two principal directions corresponding to $n = 2$ modes. On the right side of figure 4, the lines show the distribution of the amplitude of motion for different azimuth angles. It can be noticed that the amplitudes at four anti-nodes are not the same due to the structural asymmetry. The orientation of the mode shape that has a lower resonant frequency (blue solid line) is aligned with the direction of asymmetry (vertical direction) and the other mode is separated by 45°. This mode shape corresponds to $n = 2$ mode of the resonator. The information about the mode shape can be utilized as an indicator of the magnitude and orientation of the imperfections.

The effects of lapping errors on the mode shapes of wineglass resonators were demonstrated by finite element analysis (FEA), and then verified experimentally. Identical wineglass resonators with different lapping angular errors were modeled by COMSOL MultiPhysics package. In the model, the thickness of the resonators was 100 μm and the outer diameter was 7 mm. The results are shown in figure 5. Yellow lines represent the fitted sinusoidal envelops of the mode shapes. When the lapping error β is zero, which corresponds to a perfect device, the amplitudes of motion at anti-nodes are the same and the orientations of the mode shapes are random due to axisymmetric nature of the device. As β increases, the mode shapes are aligned with the direction of lapping imperfection, which is the y-axis in this model, and they deviate from the

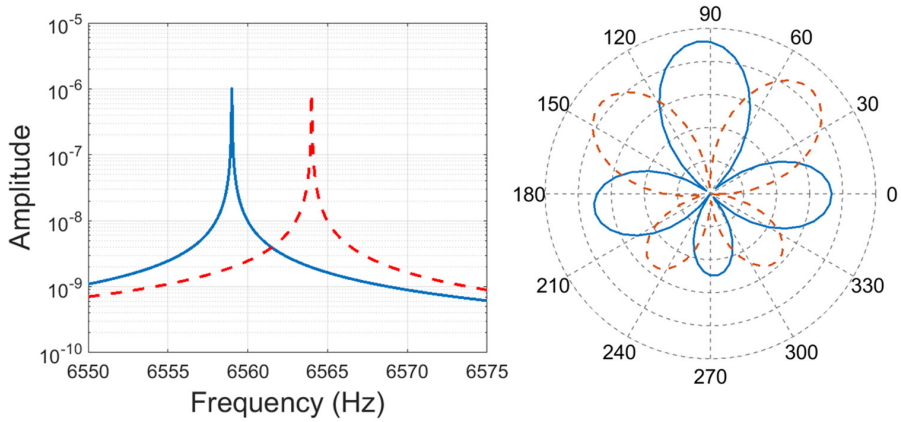

Figure 4. Effects of fabrication imperfections on the resonant frequency and mode shape ($n = 2$ in this case) of the wineglass resonator. © (2017) IEEE. Reprinted, with permission, from [22].

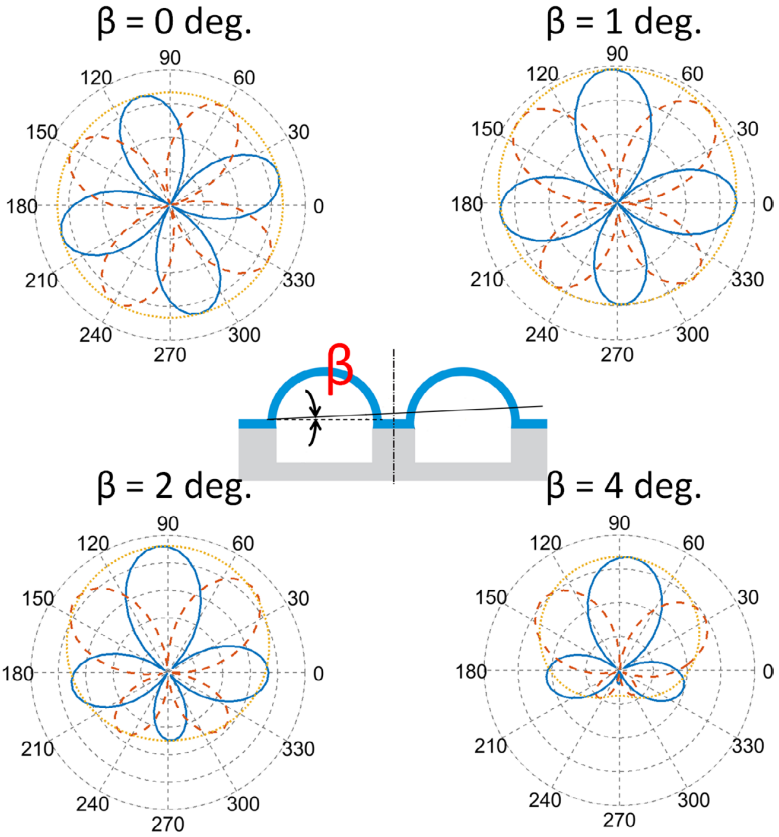

Figure 5. The effects of lapping angle on the mode shape of the wineglass resonator. Solid blue lines and dashed red lines are the azimuth amplitude distribution of the mode shapes. Yellow dotted lines are the sinusoidal envelops of the mode shapes. © (2017) IEEE. Reprinted, with permission, from [22].

case in which the amplitudes at anti-nodes are the same. It is also noticed that the azimuth amplitude of the mode shapes still follows the sinusoidal distribution. The ratio between the largest amplitude and the smallest amplitude of the sinusoidal envelop increases as β increases. The relation between the lapping angle and the ratio of amplitudes is presented in figure 6, which shows an exponential relation between the angular lapping error β and the amplitude ratio. This relation not only helps to evaluate the deviated mode shape of the structure in the frequency split model, but also allows to estimate the lapping angle needed in our algorithm to compensate for the structural asymmetry of a wineglass resonator.

2.3. Directional lapping analysis

The idea of directional lapping is to adjust structural asymmetry of the as-fabricated asymmetric structure by lapping the rim of the shell to compensate for the structural asymmetry. In

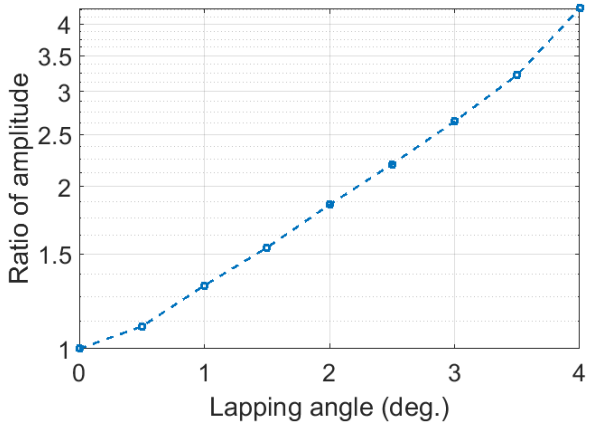

Figure 6. Exponential relation between the lapping angle and the ratio between the largest amplitude and the smallest amplitude of the sinusoidal envelop of mode shapes for the wineglass resonator. © (2017) IEEE. Reprinted, with permission, from [22].

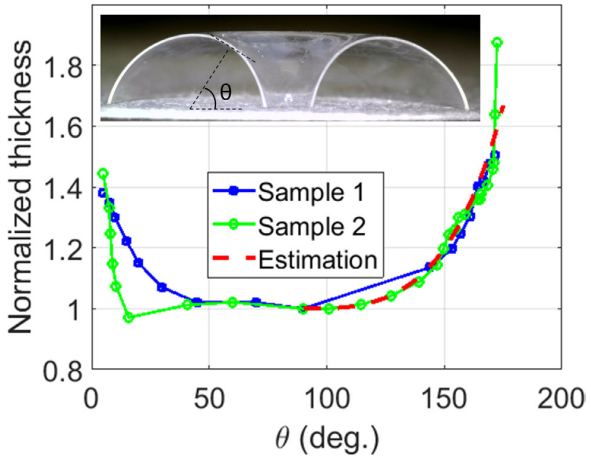

Figure 7. The cross section of the device and the thickness distribution of two samples. Structural thickness was normalized with respect to the thickness of the wineglass at the top.

this section, a model is derived to fully understand the effects of directional lapping on the structural asymmetry.

Mode shape of an ideal hemi-toroidal wineglass resonator was analytically derived based on the inextensional assumption, [21]. For asymmetric shells, deviations of mode shapes from the ideal case due to lapping errors were reported in [22]. Therefore, to numerically estimate the frequency split due to lapping errors, not only the region of integration need to be adjusted, as reported in [19], but also the deviations of the mode shapes need to be considered in the model. During the release step, the lapping will not stop precisely in the desirable location when the structure is released. This is called overlapping of the shell and will influence the frequency of the devices. In our analysis, overlapping and the thickness variation of the shell along radial direction were considered:

(1) Mode shape deviation was the most dominant factor in the frequency split analysis. It was assumed that the amplitude distribution along the radial direction remained the same as in an ideal shell, while the amplitude distribution along the tangential direction was sinusoidal with respect to the azimuth angle. The ratio between the largest amplitude and the smallest amplitude of the mode shape depends on the lapping error and follows the relation presented in figure 6.

(2) Thickness variation of the structure was inevitable in the glassblowing process since the stretching of the material was much greater at the top of the shell than around the rim. Therefore, the thickness at the rim of the structure was much larger than at the top. As a result, the lapping analysis would yield smaller effects if a uniform thickness was assumed. To develop a more accurate model, two devices were vertically lapped and their thickness distributions were measured. The experimental results are shown in figure 7. The horizontal axis is the θ angle, as shown in the figure, and the vertical axis is the normalized structural thickness with respect to the thickness at the top of the shell. Thickness distributions of the two devices matched each other well. The thickness distribution showed a thinner structure at the top and a thicker structure at the stem and rim of the shell. Only the outer part, corresponding to $\theta > 90°$, of the wineglass thickness was estimated, since the amplitude of motion is close to zero for the inner part, [21]. We applied the following function to fit the curve:

$$t = t_0 * \exp((\theta - 90)^3/1.2 \times 10^6), \quad (1)$$

where t_0 is the thickness of the wineglass at the top.

(3) Overlapping of the structure was another factor that affected the frequency split prediction. A moderate overlapping was necessary to make sure the rim of the wineglass is still in a plane. Therefore, 50 μm of overlapping was assumed for each lapping process.

Frequencies of two $n = 2$ modes were calculated based on the Rayleigh's energy method, [23]. The process was discussed in detail in [21]. In this model, the structural thickness at the top of the wineglass was assumed to be 70 μm and the outer diameter was 7 mm, matching the experimentally tested devices. The results correlating the angular lapping error and the frequency split are shown in figure 8. A good match was achieved between the model and experimental results. Around 50 Hz frequency split was induced by 3° of lapping error, i.e. 3° of directional lapping would have the capability of compensating the frequency split on the order of 50 Hz, since the directional lapping process could be considered as a reverse process of lapping error. Figure 8 also showed that the frequency split of the wineglass resonator was less sensitive to lapping errors, when the errors were small. This indicated that the directional lapping process would become more robust to errors, such as misalignment, as the frequency split was reduced. Less than 10 Hz of frequency split would be easily achieved if the error of lapping angle is controlled within 1°. This would greatly facilitate the subsequent electrostatic fine tuning of the wineglass resonators.

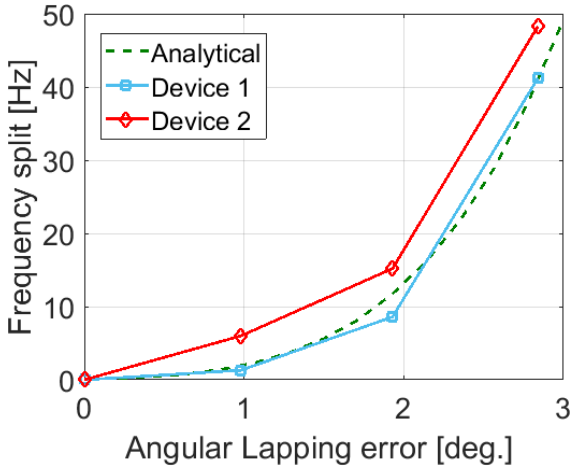

Figure 8. Relation between the angular lapping error and the frequency split of the wineglass resonator. A good match between the model and experimental results was achieved. We originally reported the experimental results in [21], and reproduced here for completeness of discussion. Reproduced with permission from [21]. Copyright © 2017 by ASME

3. Directional lapping and frequency split

There are two steps in the directional lapping to reduce the frequency split of a micro wineglass resonator. The first step is to determine the orientation of asymmetry by measuring the mode shapes of the resonator. (In this study we focused on $n = 2$ mode, but higher order modes could be considered as well). In the second step, the permanent tuning is performed by directional lapping based on the information about asymmetry of the structure.

3.1. Asymmetry identification

If we take the amplitudes of two degenerate modes as variables, 3D micro glassblown resonator vibrating in $n = 2$ wineglass modes can be modeled as a 2 degree-of-freedom system, although it is a continuous structure instead of a lumped mass-spring system. In the mode of oscillation, two principal axes of elasticity (PAE) can be identified, where the frequency of vibration will be the lowest if orientation of the mode shape is aligned with one of the PAE, and the frequency will be the highest if the mode shape is aligned with the second PAE. Since $n = 2$ wineglass mode is the most commonly used mode in 3D axisymmetric resonator gyroscopes, we only consider the PAE of $n = 2$ mode in this study.

An experimental setup was developed to determine the orientation of PAE, and it is shown in figure 9. The wineglass resonator was temporarily attached to a piezo stack by Field's metal, allowing to actuate the device during the process of parameter identification. Then, the device with the piezo stack was attached to a rotary stage, which was controlled by a servo-motor. The device was excited by piezo along the stem of the wineglass resonator and its response to actuation was measured by laser Doppler vibrometer (LDV), pointed to the outer edge of the wineglass resonator. The rotary stage was rotated by 10° after each measurement, so that the amplitude

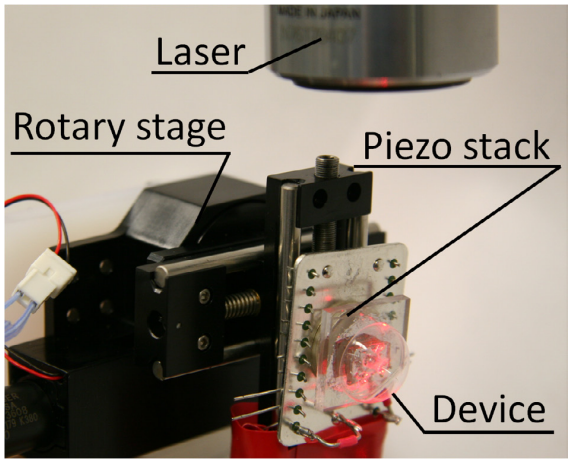

Figure 9. Experimental setup to determine the orientation of PAE of the wineglass resonator. © (2017) IEEE. Reprinted, with permission, from [22].

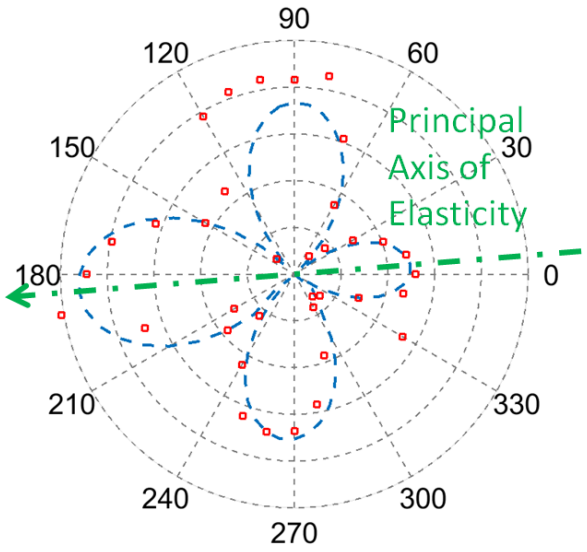

Figure 10. Experimental result of the mode shape of the wineglass resonator and the identification of PAE. © (2017) IEEE. Reprinted, with permission, from [22].

at different azimuth angles was measured to obtain the full information about the mode shape. This step of the experiment was conducted in air since the quality factor was not a critical parameter in this step. The quality factor of the resonator in the air was on the order of hundred, corresponding to a damping ratio of smaller than 0.01. Therefore, the effects of the possible asymmetric damping on the shift of modes could be neglected.

The in-plane amplitude of motion along the outer edge of the device is shown in figure 10. Red dots are the experimental results and the blue dashed line is the fitted curve. A principal axis of elasticity for $n = 2$ mode was identified according to the mode shape and is shown by a green dashed arrow. The arrow also shows the orientation of the structural asymmetry, and therefore, the anticipated directional lapping should be aligned with this direction to compensate for the structural asymmetry.

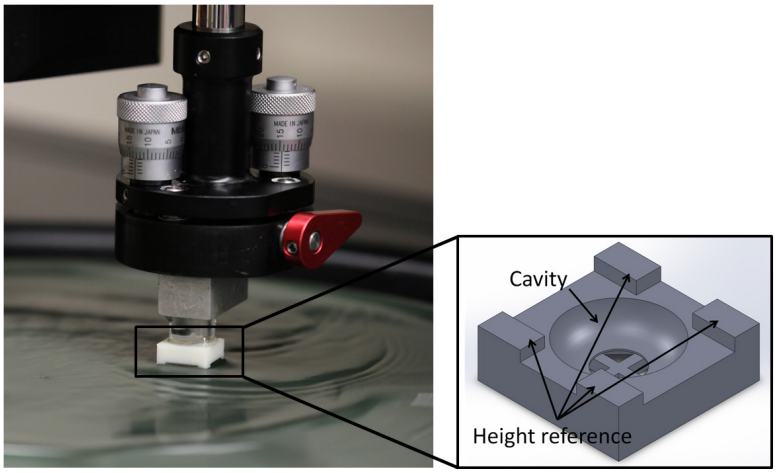

Figure 11. Experimental setup to conduct the directional lapping of the wineglass resonator and a SolidWorks model of the lapping fixture. © (2017) IEEE. Reprinted, with permission, from [22].

3.2. Asymmetry reduction

In this section, we demonstrate that the directional lapping can be utilized for reduction of asymmetry in wineglass resonators.

Special lapping fixtures were designed and 3D printed to perform the directional lapping. These fixtures were designed so that 1° of the lapping angle could be introduced by each iteration of lapping. The principal axes of elasticity was measured again after each iteration of lapping to compensate for any possible misalignment between the original PAE and the orientation of lapping in the previous iteration. The angular misalignment with our current setup is estimated to be less than 10° and possible error sources include LDV measurements of the amplitude, fabrication of lapping fixtures, and attachment of the device to the lapping fixture. The iterations of measuring and lapping make the whole process less sensitive to these possible errors than directly measuring and lapping the device just once. During the directional lapping, one side of the wineglass resonator would get contact to the lapping film and be lapped first. To be able to apply the out-of-plane electrode architecture (illustrated in figure 1), a moderate overlapping was necessary to make sure the rim of the wineglass is still in a plane, even though it may affect the efficiency of the whole process. A solid model of the fixture is shown in figure 11. The cavity in the middle of the fixture was designed to hold the device and four height references were designed to precisely control the lapping angle. Mounting of the device to the lapping fixture was described in detail in [19]. The vertical resolution of the 3D printer was within 30 μm, corresponding to about 0.1° of the lapping angle, and thus it guaranteed the control of the lapping angle with the step accuracy of 0.1°. The directional lapping process was exactly the same as the shell release process, figure 11, except that it utilized the designed fixture for directional lapping. The described process does not reduce the quality factor of the device after the compensation since the same level of surface roughness was achieved as in the release process (less than 1 nm Sa).

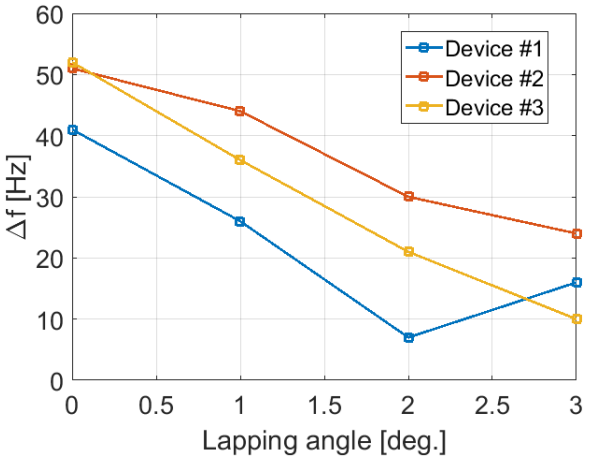

Figure 12. Experimental results demonstrating the directional lapping on three samples of wineglass resonators. The same trend of frequency split reduction was observed, confirming feasibility of the method. © (2017) IEEE. Reprinted, with permission, from [22].

After the directional lapping, the devices were cleaned by solvent and RCA-1, and characterized in the vacuum chamber by LDV to show the reduction of frequency split. Then, the identification of asymmetry was conducted again and another directional lapping was applied to the device along the updated direction of PAE to further reduce the frequency split of the device, until the frequency split reached its minimum. The goal of the subsequent identification of PAE was to compensate for any possible errors introduced by the previous directional lapping process which may arise, for example, due to the misalignment between the direction of asymmetry and the direction of lapping.

3.3. Directional lapping results

Three devices with initial frequency splits of around 50 Hz were used to illustrate results of this study. Figure 12 shows initial results of directional lapping, illustrating the same trend of frequency split reduction due to lapping along the

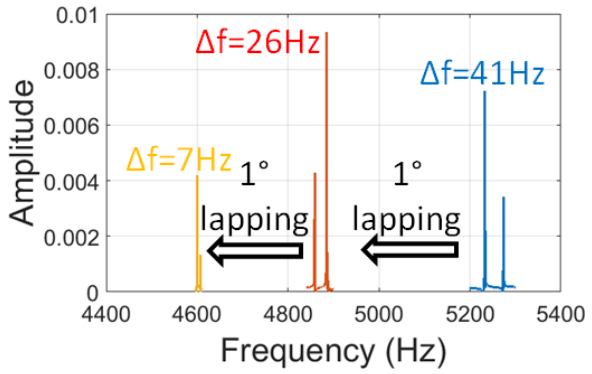

Figure 13. A near six times of frequency split reduction was demonstrated after 2° of directional lapping, reducing the frequency split from 41 Hz to 7 Hz. © (2017) IEEE. Reprinted, with permission, from [22].

PAE, and thus revealing feasibility of the method. Note that the frequency split of device #1 was increased after the third directional lapping, indicating that the frequency split of the device reached minimum when the lapping angle was between 2° and 3°. Our best result was achieved on the device #1, as showed in figure 12. A near six times of frequency split reduction was demonstrated after 2° of directional lapping by reducing the frequency split from 41 Hz to 7 Hz, as presented in figure 13. The resonant frequency of the device was also reduced from 5.2 kHz to 4.6 kHz during the process.

Figure 10 shows the amplitude of motion at the outer edge of the device #1 before compensation. The ratio between the largest amplitude of anti-node of the fitted curve (around 4.5) and the smallest amplitude of anti-node (around 2.5) was 1.8. According to figure 6, the ratio of 1.8 corresponds to the lapping angle of about 2°. This agrees with the experimental result that the frequency split was reduced to the minimum for lapping angle between 2° and 3°. The close match between the prediction and the experimental result verified the relation between the ratio of amplitudes and the lapping angle, which was derived from finite element analysis.

Another advantage of the directional lapping method is that this method is based on the mechanical lapping process, and as a result, it is compatible with most materials and no special design of the structure is needed to apply the compensation. The directional lapping method can be applied not only to fused quartz wineglass resonators, but also to almost all kinds of micro-scale 3D structures.

4. Directional lapping and quality factor

The directional lapping process is based on the mechanical lapping process. Therefore, no additional energy loss mechanism, such as surface losses, would be introduced due to the directional lapping process. Higher structural symmetry after compensation would lead to smaller loss of energy to the substrate through the anchor, and therefore, the directional lapping process is hypothesized not to reduce the overall quality factor of the wineglass resonators. The effects of thermo-elastic damping (TED) are also analyzed in this section.

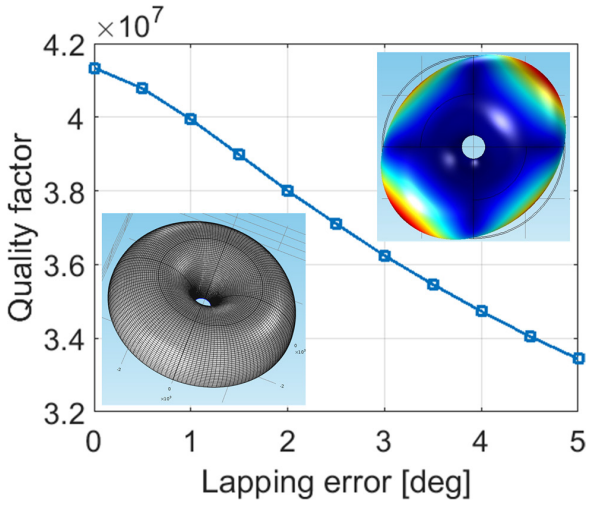

Figure 14. Relation between the lapping angle and TED limit of the resonator. Meshing and the mode shape of the wineglass resonator are also presented. The quality factor drops from 41.3 million to 33.4 million with 5° of lapping error.

4.1. Thermo-elastic damping analysis

Thermoelastic damping is an intrinsic material damping due to the coupling between the elastic field in the structure caused by deformation and the temperature field. This phenomenon is first studied in [24]. Energy is dissipated as a result of the irreversible heat flow driven by the temperature gradient caused by the deformation of a resonator. It is believed that TED is one of the dominant factors that limit the overall quality factor of a fused quartz wineglass resonator [7].

In this study, we analyzed the effects of directional lapping on TED by COMSOL MultiPhysics package. Thermoelastic damping of wineglass resonators with different lapping angles was simulated at room temperature (300 K). Dimensions of the resonators were the same as described in previous section. The results are shown in figure 14. The quality factor dropped from 41.3 million to 33.4 million after 5° of lapping error was introduced. Since directional lapping is a process of reducing the lapping errors, quality factor of wineglass resonator was expected to increase after the directional lapping procedure.

4.2. Anchor loss analysis

In physical resonators, one of the vibratory energy dissipation mechanisms is due to acoustic energy radiation into the supporting substrate through anchors during vibration. This energy loss mechanism is called the anchor loss. A numerical technique called perfectly matched layer (PML) is frequently used for modeling of resonating MEMS, [25]. The method is based on modeling the boundary of the substrate, which can perfectly absorb the acoustic waves triggered by vibration of the resonator, resulting in an upper bound of anchor loss. The anchor loss prediction by this approach showed a good agreement with experimental results, for example in [26]. To make sure that PML could completely absorb the vibratory energy while keeping a tractable amount of calculation, the

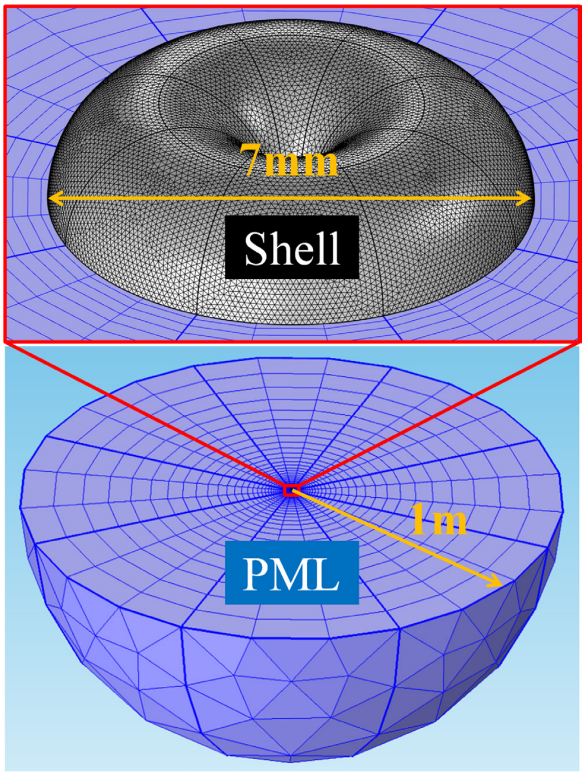

Figure 15. COMSOL MultiPhysics package was used to calculate the anchor loss. The blue region is the PML and the gray region is the device. Varying mesh distribution in the PML is also shown.

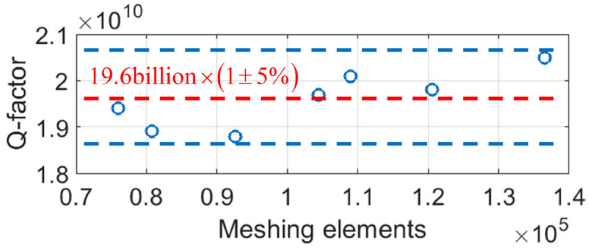

Figure 16. Relation between the meshing element number and the FEM results. Mesh elements, varied from 7.59×10^4 to 1.37×10^5, confirmed the convergence of the model with a tolerance of 5%.

thickness of the PML should be the same as the wavelength of the acoustic wave propagated through the substrate, [27].

In this study, we applied the PML approach to study the effects of directional lapping on anchor losses of the wineglass resonators by COMSOL MultiPhysics package. Hemispherical PML with a device at its center was highly effective in absorbing acoustic waves in the radial direction, [27], and therefore it was chosen for this study. The working frequencies of the resonators were between 5 and 10 kHz. The wavelength of the acoustic wave generated by the vibration of the resonator in the glass substrate was less than 1 m. Therefore, we set the radius of PML to be 1 m. Dimensions of the devices were the same as described in previous section. Details of the model are presented in figure 15. The size of the PML is much larger than the actual size of the substrate due to

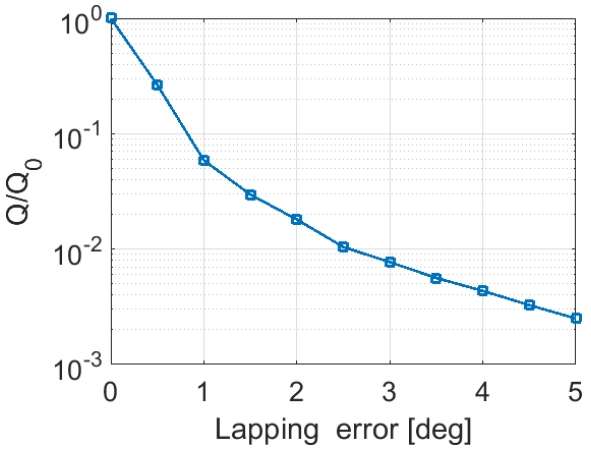

Figure 17. Relation between the lapping angle and the quality factor due to anchor loss of wineglass resonators. A 400 times reduction in the quality factor due to anchor loss was numerically predicted with 5° of lapping error.

Table 1. Surface roughness of rim of the shell before and after compensation.

	Surface roughness Sa (nm)				
Sample status	Point 1	Point 2	Point 3	Point 4	Average
Before lapping	0.75	0.85	1.18	0.76	0.89
After lapping	1.17	0.64	0.92	0.70	0.86

the relatively low resonant frequency of the device. It does not contradict with the real case since the function of PML is just to fully absorb the vibration and it does not correspond to any physical object in the experimental setup.

Meshing quality was critical in this study since the dimensions of the device (70 μm in thickness) were 3–4 orders of magnitude smaller than those of the PML (1 m in radius). The shell geometry was discretized with tetrahedron meshing elements of the size on the order of 50 μm. Meshing distribution inside PML, however, changed from very small elements in the region close to the shell geometry (on the order of 100 μm) to very large elements at the boundary (around 0.2 m). The ratio of the size of the largest element to the smallest element was 2000 in this model.

Anchor loss of an ideal axisymmetric wineglass resonator was first calculated. The quality factor due to anchor loss was 19.6 billion and it was referred as Q_0 in this paper. Mesh elements, varied from 7.59×10^4 to 1.37×10^5, confirmed the convergence of the model with a tolerance of 5%, figure 16. Then, angular lapping errors were introduced in the shell structure and the quality factor was calculated again. The relation between the quality factor and lapping error is shown in figure 17. A 400 times of reduction in the quality factor due to anchor loss was numerically demonstrated with 5° of lapping error. Since directional lapping process was the inverse of the lapping error process, the increase in quality factor due to the anchor loss was expected. However, due to the balanced nature of the structure, the quality factor limit due to the anchor loss was much higher than the TED limit of the device. Therefore,

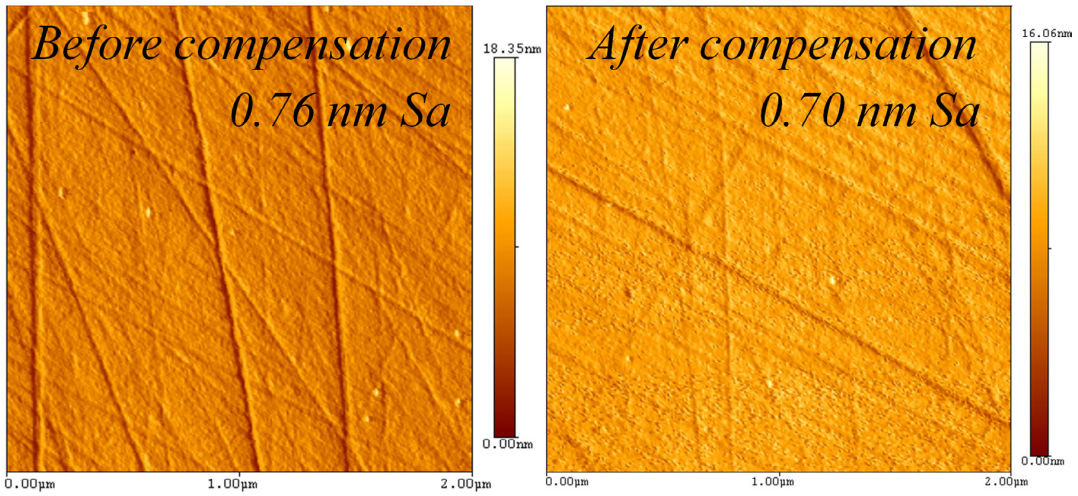

Figure 18. AFM images of the surface of wineglass rim before and after compensation.

the increase of the overall quality factor due to lapping was not expected to be observed experimentally.

4.3. Surface finish analysis

Surface loss is another important factor that affects the quality factor of the wineglass resonator. The surface roughness has been demonstrated to influence the surface loss, [28]. To eliminate the effect from our experiments, we kept the surface roughness of rim of the devices the same after the compensation process, in order to keep the surface loss constant.

The directional lapping process is based on the mechanical removal of the material as in the mechanical lapping process. As a result, the surface finish at the rim will not be degraded after the compensation process and the overall quality factor will not be affected. To experimentally prove this conclusion, the surface roughness of the rim of a wineglass resonator was measured before and after the directional lapping process. Atomic force microscope (AFM) from Pacific Nanotechnology (Nano-R) was used to measure the surface roughness of the samples. The scan area was selected to be 2 μm $\times$ 2 μm. Four different points on the rim were measured and the average was calculated. The sample was cleaned by standard solvent cleaning (acetone, isopropanol, and methanol) before each scan. The AFM was run in a close contact mode, using a 10 nm radius probe tip (Agilent U3120A). The results are listed in table 1. The average surface roughness was 0.89 nm and 0.86 nm before and after directional lapping process, respectively. No obvious surface roughness changes were observed. AFM images before and after the compensation procedure are shown in figure 18. Trenches with the depth of around 10 nm were observed in both measurements, indicating a similar level of surface finish.

5. Conclusion

The directional lapping process was proposed and experimentally demonstrated as a frequency split reduction method. Near six times of frequency split reduction, from 41 Hz to 7 Hz, was demonstrated on fused quartz wineglass resonators. Surface finish of the device after the compensation remained the same as before compensation, indicating that the process did not degrade the overall quality factor of the resonators.

In this paper, a glassblowing model was first developed to predict the effects of non-uniform temperature during the glassblowing on structural asymmetry. Then, a semi-analytical model was derived to verify the feasibility of directional lapping on the frequency split reduction. In the directional lapping process, the structural asymmetry was first identified by measuring the mode shape of a resonator. Then, the directional lapping was conducted to reduce the asymmetry, and therefore, the frequency split of the device. The energy dissipation mechanisms, such as anchor loss and surface loss, were analyzed to prove the ability of this approach for reduction of asymmetry, without causing losses in the quality factor despite the introduction of additional lapping steps.

In this paper, for the first time, we introduced and experimentally demonstrated a process for permanent structural compensation of the frequency split of 3D shell structures. We showed that the process is naturally integrated in our fabrication sequence, and confirmed that the additional step does not result in degradation of the quality factor. This process is envisioned as a step in the three-step fabrication and tuning sequence, where a precision shell is fabricated, directionally lapped, and finally electrostatically fine-tuned.

Acknowledgment

This material is based upon work supported by the DARPA grant W31P4Q-11-1-0006. Devices were designed and tested in the MicroSystems Lab of the University of California, Irvine. Fabrication of the devices was performed at the Integrated Nanosystem Research Facility (INRF) of the University of California, Irvine.

ORCID iDs

Yusheng Wang https://orcid.org/0000-0003-0532-4859

References

[1] Rozelle D M 2009 The hemispherical resonator ryro: from wineglass to the planets *Proc. 19th AAS/AIAA Space Flight Mechanics Meeting (Savannah, GA, USA, 8–12 February 2009)*

[2] Trusov A A, Phillips M R, Bettadapura A, Atikyan G, McCammon G H, Pavell J M, Choi Y A, Sakaida D K, Rozelle D M and Meyer A D 2016 mHRG: miniature CVG with beyond navigation grade performance and real time self-calibration *IEEE Int. Symp. on Inertial Sensors and Systems (Laguna Beach, CA, USA, 22–25 February 2016)*

[3] Matthews A and Bauer D A 1995 Hemispherical resonator gyro noise reduction for precision spacecraft pointing *Space Guidance, Control, and Tracking II (Orlando, FL, USA, 12 June 1995)*

[4] Shao P, Mayberry C L, Gao X, Tavassoli V and Ayazi F 2014 A polysilicon microhemispherical resonating gyroscope *IEEE/ASME J. Microelectromech. Syst.* **23** 762–4

[5] Bernstein J J *et al* 2015 High Q diamond hemispherical resonators: fabrication and energy loss mechanisms *J. Micromech. Microeng.* **25** 085006

[6] Kanik M, Bordeenithikasem P, Kim D, Selden N, Desai A, M'Closkey R and Schroers J 2015 Metallic glass hemispherical shell resonators *IEEE/ASME J. Microelectromech. Syst.* **24** 19–28

[7] Senkal D, Ahamed M J, Asadian M H, Askari S and Shkel A M 2015 Demonstration of 1 million Q-factor on microglassblown wineglass resonators with out-of-plane electrostatic transduction *IEEE/ASME J. Microelectromech. Syst.* **24** 29–37

[8] Cho J, Woo J-K, Yan J, Peterson R L and Najafi K 2014 Fused silica micro birdbath resonator gyroscope *IEEE/ASME J. Microelectromech. Syst.* **23** 66–77

[9] Shkel A M 2006 Type I and type II micromachined vibratory gyroscopes *IEEE/ION Position, Location, and Navigation Symp. (San Diego, CA, USA, 25–27 April 2006)*

[10] Gallacher B J, Hedley J, Burdess J S, Harris A J, Rickard A and King D O 2005 Electrostatic correction of structural imperfections present in a microring gyroscope *IEEE/ASME J. Microelectromech. Syst.* **14** 221–34

[11] Kim D J and M'Closkey R T 2006 A systematic method for tuning the dynamics of electrostatically actuated vibratory gyros *IEEE Trans. Control Syst. Technol.* **14** 69–81

[12] Asadian M H, Wang Y, Askari S and Shkel A M 2017 Controlled capacitive gaps for electrostatic actuation and tuning of 3D fused quartz micro wineglass resonator gyroscope *IEEE Int. Symp. on Inertial Sensors and Systems (Kauai, HI, USA, 27–30 March 2017)*

[13] Rourke A K, McWilliam S and Fox C H J 2001 Multi-mode trimming of imperfect rings *J. Sound Vib.* **248** 695–724

[14] Gallacher B J, Hedley J, Burdess J S, Harris A J and McNie M E 2003 Multimodal tuning of a vibrating ring using laser ablation *Proc. Inst. Mech. Eng. Part C: J. Mech. Eng. Sci.* **217** 557–76

[15] Schwartz D M, Kim D, Stupar P, DeNatale J and M'Closkey R T 2015 Modal parameter tuning of an axisymmetric resonator via mass perturbation *IEEE/ASME J. Microelectromech. Syst.* **24** 545–55

[16] Viswanath A, Li T and Gianchandani Y 2014 High resolution micro ultrasonic machining for trimming 3D microstructures *J. Micromech. Microeng.* **24** 065017

[17] Trusov A, Senkal D and Shkel A M 2015 Microfabrication of high quality three dimensional structures using wafer-level glassblowing of fused quartz and ultra low expansion glasses *US Patent* 9,139,417

[18] Senkal D, Ahamed M J, Trusov A A and Shkel A M 2013 High temperature micro-glassblowing process demonstrated on fused quartz and ULE TSG *Sensors Actuators* A **201** 525–31

[19] Wang Y, Asadian M H and Shkel A M 2016 Predictive analytical model of fundamental frequency and imperfections in glassblown fused quartz hemi-toroidal 3D micro shells *IEEE Sensors Conf. (Orlando, FL, USA, 30 October–2 November 2016)*

[20] Doremus R H 2002 Viscosity of silica *J. Appl. Phys.* **92** 7619–29

[21] Wang Y, Asadian M H and Shkel A M 2017 Modeling the effect of imperfections in glassblown micro-wineglass fused quartz resonators *ASME J. Vib. Acoust.* **139** 040909

[22] Wang Y, Asadian M H and Shkel A M 2017 Frequency split reduction by directional lapping of fused quartz micro wineglass resonators *IEEE Int. Symp. on Inertial Sensors and Systems (Kauai, HI, USA, 27–30 March 2017)*

[23] Rayleigh J W S B 1896 *The Theory of Sound* vol 2 (London: Macmillan)

[24] Zener C 1937 Internal friction in solids. I. Theory of internal friction in reeds *Phys. Rev.* **52** 230

[25] Weinberg M, Candler R, Chandorkar S, Varsanik J, Kenny T and Duwel A 2009 Energy loss in MEMS resonators and the impact on inertial and RF devices *Solid-State Sensors, Actuators and Microsystems Conf. (Denver, CO, USA, 21–25 June 2009)*

[26] Judge J A, Photiadis D M, Vignola J F, Houston B H and Jarzynski J 2007 Attachment loss of micromechanical and nanomechanical resonators in the limits of thick and thin support structures *J. Appl. Phys.* **101** 013521

[27] Darvishian A, Shiari B, Cho J Y, Nagourney T and Najafi K 2017 Anchor loss in hemispherical shell resonators *IEEE/ASME J. Microelectromech. Syst.* **26** 51–66

[28] Wang Y and Shkel A M 2016 Study on surface roughness improvement of fused quartz after thermal and chemical post-processing *IEEE Int. Symp. on Inertial Sensors and Systems (Laguna Beach, CA, USA, 22–25 February 2016)*